Journal of the Physical Society of Japan **86**, 101013 (2017)
https://doi.org/10.7566/JPSJ.86.101013

Hydrodynamic Effects in Oscillatory Active Nematics

Alexander S. Mikhailov[1,2*], Yuki Koyano[3], and Hiroyuki Kitahata[3]

[1]*Abteilung Physikalische Chemie, Fritz-Haber-Institut der Max-Planck-Gesellschaft, 14195 Berlin, Germany*
[2]*Department of Mathematical and Life Sciences, Hiroshima University, Higashihiroshima, Hiroshima 739-8526, Japan*
[3]*Department of Physics, Chiba University, Chiba 263-8522, Japan*

(Received February 28, 2017; accepted March 21, 2017; published online August 25, 2017)

Oscillatory active nematics represent nonequilibrium suspensions of microscopic objects, such as natural or artificial molecular machines, that cyclically change their shapes and thus operate as oscillating force dipoles. In this mini-review, hydrodynamic collective effects in such active nematics are discussed. Microscopic stirring at low Reynolds numbers induces non-thermal fluctuating flows and passive particles become advected by them. Similar to advection of particles in macroscopic turbulent flows, this enhances diffusion of tracer particles. Furthermore, their drift and accumulation in regions with stronger activity or higher concentration of force dipoles take place. Analytical investigations and numerical simulations both for 2D and 3D systems were performed.

1. Introduction

Nematics are formed by elongated molecules. When temperature is decreased, they undergo a phase transition to a liquid-crystalline state where the molecules are orientationally ordered, but the translational order is absent and the system remains fluid.[1)] For classical nematics, the shapes of the molecules are fixed (or only subject to equilibrium thermal fluctuations). There are however important applications where active nematics with the elements that cyclically change their shape have to be analyzed.

First of all, this situation is encountered when the elements represent molecular machines, either natural or artificial.[2,3)] The characteristic property of a machine is that, in each operation cycle, it repeatedly changes its conformation, powered by the energy that is externally supplied. Protein machines, acting as motors, enzymes, ion pumps, or performing operations with other biomolecules, constitute a fundamental component of the living cell; typically they are driven by the energy released in the hydrolysis of ATP. On the other hand, it becomes also possible to design and synthesize non-biological molecules that behave as machines, with the energy supplied by illumination or in a chemical way.[4,5)] Investigations of artificial molecular machines is a rapidly developing field. Molecular machines can be incorporated into liquid crystals (see, e.g., the experiments[6)]), so that their orientational ordering is induced. Moreover, under crowded conditions that are characteristic for biological cells, they can undergo an orientational ordering transition and produce liquid crystals themselves. Note that, in such a liquid crystal, the molecules are active and cyclically elongate or contract.

A different class of oscillatory active nematics is constituted by bacteria and other microorganisms. It is well known that a biological cell may actively change its shape and this can result in the swimming effect.[7)] However, one can also imagine microorganisms that do not propel themselves, but just repeatedly change their shapes in a reciprocal way. Again, such microorganisms may undergo an orientational ordering transition, either as a result of crowding or external condition.

Moreover, these active nematics can be manufactured too. Indeed, one can prepare oscillating dumbbells where the distance between two beads is cyclically changed through application of an external periodic field or due to other effects. Such dumbbells can form orientationally ordered states as well.

Whereas the nature of the considered active nematics may vary, there are common properties shared by all of them. From the hydrodynamical point of view, almost any object immersed into a fluid and changing its shape represents a force dipole.[8)] Thus, one needs to consider hydrodynamic effects in large populations of active force dipoles.

Previously, such hydrodynamical effects have been analyzed assuming that the orientational ordering of active force dipoles was absent.[9)] It has been shown that, even in this case, diffusion of passive tracer particles becomes enhanced and, if concentration or activity gradients for force dipoles are created, directed drift of tracer particles takes place.[9,10)] Detailed investigations were performed for two-dimensional systems, such as biomembranes with active protein inclusions,[11)] and the effects in viscoelastic three-dimensional media were also analyzed.[12)] In this article, we construct a general theory for hydrodynamic effects of orientationally ordered active force dipoles and illustrate it by numerical simulations for several selected set-ups. We also briefly review the previous results for disordered force dipoles. Our approach is general and therefore the analysis is applicable not only for biological systems, but also for the synthetic and artificial machines.

2. Populations of Oscillating Force Dipoles

The system that we consider in this study represents a population of microscopic objects that cyclically change their shape and are immersed into a viscous fluid. We assume that hydrodynamic flows induced by such oscillating objects are characterized by low Reynolds numbers, so that inertia is absent and the Navier–Stokes equations can be linearized. Our aim is to determine the intensity and statistical properties of non-thermal flow velocity fluctuations caused by the active elements.

It is known that, at a distance much longer than its size, any object that asymmetrically changes its shape can generally be described as a force dipole. The force dipole i is characterized by its position $\boldsymbol{R}_i$, its orientation unit vector $\boldsymbol{e}_i$ and its magnitude m_i. For example, if the object represents a dumbbell that cyclically changes its length,[9)] the magnitude of its force dipole is $m = Fl_{\mathrm{fd}}$ where l_{fd} is the distance

between the two beads and F is the force acting between them. Note that the magnitude m of the force dipole can be positive or negative, depending on whether there are repulsive or attractive forces between the beads.

Because inertia is absent on the considered length and time scales, the flows are instantaneously following changes in the force dipoles. The flow velocity $\boldsymbol{v}$ at point $\boldsymbol{R}$ is given by (here and below, summation over repeated indices is always assumed)

$$v_\alpha(\boldsymbol{R}) = \sum_i \frac{\partial G_{\alpha\beta}(\boldsymbol{R}-\boldsymbol{R}_i)}{\partial R_\gamma} e_{i,\beta} e_{i,\gamma} m_i, \tag{1}$$

where $G_{\alpha\beta}(\boldsymbol{r})$ is the Green's function of the Navier–Stokes equations,

$$G_{\alpha\beta}(\boldsymbol{r}) = \frac{1}{8\pi\mu r}\left(\delta_{\alpha\beta} + \frac{r_\alpha r_\beta}{r^2}\right), \quad \text{for } d=3, \tag{2}$$

$$G_{\alpha\beta}(\boldsymbol{r}) = \frac{1}{4\pi\mu}\left[-(1+\ln r) + \frac{r_\alpha r_\beta}{r^2} + \text{const.}\right], \quad \text{for } d=2, \tag{3}$$

with μ being the fluid viscosity. Note that μ is the bulk viscosity for $d=3$ and the surface viscosity for $d=2$, and therefore the dimensions of these two properties are different.

The expression (1) is invariant with respect to the reflection $\boldsymbol{e} \to -\boldsymbol{e}$. Hence, although we can assign a unit orientation vector to a force dipole, its direction (positive or negative) is irrelevant. This means that a force dipole is characterized, like an elongated molecule in a nematic liquid crystal, by specifying only its director line.

To avoid the ambiguity involved in the choice of vectors $\boldsymbol{e}$, a nematic orientation tensor $N^d_{i,\beta\gamma}$ for the force dipole i can be introduced,

$$N^d_{i,\beta\gamma} = e_{i,\beta} e_{i,\gamma} - \frac{1}{d}\delta_{\beta\gamma}. \tag{4}$$

In terms of this tensor, the velocity field can be equivalently expressed as

$$v_\alpha(\boldsymbol{R}) = \sum_i \frac{\partial G_{\alpha\beta}(\boldsymbol{R}-\boldsymbol{R}_i)}{\partial R_\gamma} m_i N^d_{i,\beta\gamma}, \tag{5}$$

where we have taken into account that the identity $\partial G_{\alpha\beta}/\partial R_\beta = 0$ holds.

If there are N force dipoles whose positions, orientations and magnitudes vary with time, and we have

$$v_\alpha(\boldsymbol{R},t) = \sum_i \frac{\partial G_{\alpha\beta}(\boldsymbol{R}-\boldsymbol{R}_i(t))}{\partial R_\gamma} m_i(t) N^d_{i,\beta\gamma}(t). \tag{6}$$

Certain assumptions about statistical properties of active force dipoles will be made: The mean magnitude of the force dipole is zero, $\langle m_i(t)\rangle = 0$, and oscillations in different force dipoles are statistically independent (i.e., incoherent), so that $\langle m_i(t) m_j(t')\rangle = 0$ for $i \neq j$. The autocorrelation function of force dipoles is

$$\langle m_i(t) m_i(0)\rangle = S(t). \tag{7}$$

In this study, we will consider two limiting cases: when the nematic order is absent and force dipoles are randomly oriented, and when all force dipoles are perfectly aligned. The intermediate situation, where both the nematic order and orientational fluctuations are present, should be a subject for further research.

When orientational order is absent, $\langle N^d_{i,\beta\gamma}(t)\rangle = 0$, we have (using the orientational symmetry)

$$\langle N^d_{i,\beta\gamma}(t) N^d_{j,\beta'\gamma'}(0)\rangle = \sigma(t)\Lambda^d_{\beta\gamma\beta'\gamma'}\delta_{ij}, \tag{8}$$

where $\sigma(t)$ is the orientational autocorrelation function, such that $\sigma(0)=1$, and

$$\Lambda^3_{\beta\gamma\beta'\gamma'} = \frac{1}{15}\left(\delta_{\beta\beta'}\delta_{\gamma\gamma'} + \delta_{\beta\gamma'}\delta_{\beta'\gamma} - \frac{2}{3}\delta_{\beta\gamma}\delta_{\beta'\gamma'}\right), \tag{9}$$

$$\Lambda^2_{\beta\gamma\beta'\gamma'} = \frac{1}{8}(\delta_{\beta\beta'}\delta_{\gamma\gamma'} + \delta_{\beta\gamma'}\delta_{\beta'\gamma} - \delta_{\beta\gamma}\delta_{\beta'\gamma'}). \tag{10}$$

In the case of perfect nematic orientational order,

$$\langle N^d_{i,\beta\gamma}(t)\rangle = \overline{N}^d_{\beta\gamma} \neq 0, \tag{11}$$

and

$$\langle N^d_{i,\beta\gamma}(t) N^d_{j,\beta'\gamma'}(0)\rangle = \overline{N}^d_{\beta\gamma}\overline{N}^d_{\beta'\gamma'}. \tag{12}$$

The tensor $\overline{N}^d_{\beta\gamma}$ is symmetric and has a vanishing trace. By solving the eigenvalue problem, one can find a coordinate frame where the tensor is diagonal and its eigenvalues are $(\lambda, \lambda_0, \lambda_0)$ with $\lambda + 2\lambda_0 = 0$, i.e., $\lambda_0 = -(1/2)\lambda$, for $d=3$. Moreover, we have $2/3 \geq \lambda \geq 0$. Hence, if $\boldsymbol{e}^0$ is a unit vector specifying the direction of the nematic order, we have

$$\overline{N}^3_{\beta\gamma} = \frac{3}{2}\lambda\left(e^0_\beta e^0_\gamma - \frac{1}{3}\delta_{\beta\gamma}\right), \quad \text{for } d=3. \tag{13}$$

In the same manner, we have

$$\overline{N}^2_{\beta\gamma} = 2\lambda\left(e^0_\beta e^0_\gamma - \frac{1}{2}\delta_{\beta\gamma}\right), \quad \text{for } d=2, \tag{14}$$

and $1/2 \geq \lambda \geq 0$. Note that λ represents the nematic order parameter.

Spatial positions $\boldsymbol{R}_i(t)$ of force dipoles can change with time. We assume that motions of the particles bearing force dipoles, represent a diffusion process. Therefore, the conditional probability density $\varphi_d(\boldsymbol{R},t)$ to find an active particle at time t (>0) at the distance R from its initial position at $t=0$ is given by

$$\varphi_d(\boldsymbol{R},t) = \frac{\zeta_d}{(Dt)^{d/2}}\exp\left[-\frac{R^2}{4Dt}\right], \tag{15}$$

where D is the diffusion coefficient and ζ_d is a numerical coefficient [$\zeta_3 = (4\pi)^{-3/2}$ and $\zeta_2 = (4\pi)^{-1}$].

Finally, Eq. (6) can be also written in the form

$$v_\alpha(\boldsymbol{R},t) = \int d\boldsymbol{r}\, \frac{\partial G_{\alpha\beta}(\boldsymbol{R}-\boldsymbol{r})}{\partial R_\gamma}\eta_{\beta\gamma}(\boldsymbol{r},t), \tag{16}$$

where

$$\eta_{\beta\gamma}(\boldsymbol{r},t) = \sum_i m_i(t) N^d_{i,\beta\gamma}\delta(\boldsymbol{r}-\boldsymbol{R}_i(t)), \tag{17}$$

is the noise representing a fluctuating force field.

In absence of orientational order, the autocorrelation function of this noise is

$$\langle \eta_{\beta\gamma}(\boldsymbol{r},t)\eta_{\beta'\gamma'}(\boldsymbol{0},0)\rangle = cS(t)\sigma(t)\varphi_d(\boldsymbol{r},t)\Lambda^d_{\beta\gamma\beta'\gamma'}. \tag{18}$$

where c is the concentration of force dipoles at the reference point $\boldsymbol{r}=\boldsymbol{0}$ and reference time $t=0$.

If the orientational order is present, we have

$$\langle \eta_{\beta\gamma}(\boldsymbol{r},t)\eta_{\beta'\gamma'}(\boldsymbol{0},0)\rangle = cS(t)\varphi_d(\boldsymbol{r},t)\overline{N}^d_{\beta\gamma}\overline{N}^d_{\beta'\gamma'}. \tag{19}$$

Equation (16), that includes the active noise $\eta_{\beta\gamma}(\boldsymbol{r},t)$, describes fluctuating flows induced by collective activity of the population of force dipoles.

3. Advection of Passive Particles Induced by Force Dipoles

A small tracer particle immersed into a fluid will always move, at low Reynolds numbers, at the same velocity as the local flow velocity of the fluid. Hence, the particle will be advected by the fluctuating flow field. If $\boldsymbol{R}(t)$ is the particle position, we have

$$\frac{dR_\alpha}{dt} = v_\alpha(\boldsymbol{R},t), \tag{20}$$

where $\boldsymbol{v}(\boldsymbol{R},t)$ is the flow velocity determined by Eq. (16).

Here, an important distinction has to be made. If we keep fixed the observation point $\boldsymbol{R}$, time average of the local fluctuating velocity field will be always zero. Indeed, for $T\to\infty$, we have

$$\frac{1}{T}\int_0^T v_\alpha(\boldsymbol{R},t)\,dt = \int d\boldsymbol{r}\,\frac{\partial G_{\alpha\beta}(\boldsymbol{R}-\boldsymbol{r})}{\partial r_\gamma}\,\frac{1}{T}\int_0^T \eta_{\beta\gamma}(\boldsymbol{r},t)\,dt \to \int d\boldsymbol{r}\,\frac{\partial G_{\alpha\beta}(\boldsymbol{R}-\boldsymbol{r})}{\partial r_\gamma}\,\langle\eta_{\beta\gamma}(\boldsymbol{r},t)\rangle = 0. \tag{21}$$

On the other hand, if $\boldsymbol{R}(t)$ is the current position of a passive tracer which is advected with the flow and moves together with it according to Eq. (20), the time average of the particle velocity $V_\alpha(t) = dR_\alpha/dt$ does not vanish. In this case,

$$\frac{1}{T}\int_0^T V_\alpha(t)\,dt = \frac{1}{T}\int_0^T v_\alpha(\boldsymbol{R}(t),t)\,dt \to \int d\boldsymbol{r}\left\langle\frac{\partial G_{\alpha\beta}(\boldsymbol{R}(t)-\boldsymbol{r})}{\partial r_\gamma}\,\eta_{\beta\gamma}(\boldsymbol{r},t)\right\rangle \neq 0 \tag{22}$$

because $\boldsymbol{R}(t)$ is correlated with the noise $\eta_{\beta\gamma}(\boldsymbol{r},t)$. Therefore, directed drift of advected particles can arise.

Thus, we expect that advection will have two effects. First, diffusion of a tracer particle will be enhanced and, second, under certain conditions the drift of a tracer particle will be induced.

Suppose that the nematic order is absent. Then, if deviations $R_\alpha(t) = R^0_\alpha + \rho_\alpha(t)$ of a tracer particle from its initial position are small, we can approximately write

$$\frac{d\rho_\alpha}{dt} = \int d\boldsymbol{r}\,\frac{\partial G_{\alpha\beta}(\boldsymbol{R}^0-\boldsymbol{r})}{\partial r_\gamma}\,\eta_{\beta\gamma}(\boldsymbol{r},t) - \rho_\delta\int d\boldsymbol{r}\,\frac{\partial^2 G_{\alpha\beta}(\boldsymbol{R}^0-\boldsymbol{r})}{\partial r_\gamma\partial r_\delta}\,\eta_{\beta\gamma}(\boldsymbol{r},t). \tag{23}$$

Using this equation, we can determine the drift velocity and the mean-square displacement of the tracer particle within a given time.

In the linear order in the noise intensity, the displacement $\boldsymbol{\rho}(T)$ from $\boldsymbol{R}^0$ within time T is

$$\rho_\alpha(T) = \int_0^T dt\int d\boldsymbol{r}\,\frac{\partial G_{\alpha\beta}(\boldsymbol{R}^0-\boldsymbol{r})}{\partial r_\gamma}\,\eta_{\beta\gamma}(\boldsymbol{r},t). \tag{24}$$

By using this expression, we find

$$\langle\rho_\alpha(T)\rho_{\alpha'}(T)\rangle_{\boldsymbol{R}^0} = \int_0^T dt_1\int_0^T dt_2\int d\boldsymbol{r}_1\int d\boldsymbol{r}_2\,\frac{\partial G_{\alpha\beta}(\boldsymbol{R}^0-\boldsymbol{r}_1)}{\partial r_{1,\gamma}} \times\frac{\partial G_{\alpha'\beta'}(\boldsymbol{R}^0-\boldsymbol{r}_2)}{\partial r_{2,\gamma'}}\,\langle\eta_{\beta\gamma}(\boldsymbol{r}_1,t_1)\eta_{\beta'\gamma'}(\boldsymbol{r}_2,t_2)\rangle. \tag{25}$$

Introducing the variables $t=(t_1+t_2)/2$, $\tau=t_1-t_2$ and $\boldsymbol{R}=(\boldsymbol{r}_1+\boldsymbol{r}_2)/2$, $\boldsymbol{r}=\boldsymbol{r}_1-\boldsymbol{r}_2$ and taking into account Eq. (18), one obtains

$$\langle\rho_\alpha(T)\rho_{\alpha'}(T)\rangle_{\boldsymbol{R}^0} = \Lambda^d_{\beta\gamma\beta'\gamma'}\int_0^T dt\int_{-2t}^{2t} d\tau\,S(\tau)\sigma(\tau) \times\int d\boldsymbol{R}\int d\boldsymbol{r}\,\frac{\partial G_{\alpha\beta}(\boldsymbol{R}^0-\boldsymbol{R}-\boldsymbol{r}/2)}{\partial R_\gamma} \times\frac{\partial G_{\alpha'\beta'}(\boldsymbol{R}^0-\boldsymbol{R}+\boldsymbol{r}/2)}{\partial R_{\gamma'}}\,c(\boldsymbol{R})\varphi_d(\boldsymbol{r},\tau), \tag{26}$$

where $c(\boldsymbol{R})$ is the concentration of force dipoles at location $\boldsymbol{R}$.

An important role in the last equation is played by the product $S(\tau)\sigma(\tau)$ of the autocorrelation functions for the magnitude and the orientation of force dipoles. This product is nonvanishing only within a certain time τ_c. Within this time, a force dipole will typically diffuse over the distance about $l=(D\tau_c)^{1/2}$ and hence the integration over $\boldsymbol{r}$ is in fact restricted to the volume element of this linear size. Assuming that the functions $G_{\alpha\beta}$ do not significantly change over the short distance l_c, we can neglect their dependence on $\boldsymbol{r}$, i.e., we can take $G_{\alpha\beta}(\boldsymbol{R}^0-\boldsymbol{R}\pm\boldsymbol{r}/2)\approx G_{\alpha\beta}(\boldsymbol{R}^0-\boldsymbol{R})$. Moreover, we can notice that $\int d\boldsymbol{r}\,\varphi_d(\boldsymbol{r},\tau)=1$. As a result, we have

$$\langle\rho_\alpha(T)\rho_{\alpha'}(T)\rangle_{\boldsymbol{R}^0} = 2\Lambda^d_{\beta\gamma\beta'\gamma'}\int d\boldsymbol{R}\,\frac{\partial G_{\alpha\beta}(\boldsymbol{R}^0-\boldsymbol{R})}{\partial R_\gamma}\,\frac{\partial G_{\alpha'\beta'}(\boldsymbol{R}^0-\boldsymbol{R})}{\partial R_{\gamma'}} \times c(\boldsymbol{R})\int_0^T dt\int_0^{2t} d\tau\,S(\tau)\sigma(\tau). \tag{27}$$

Note that because of the identity

$$\delta_{\beta\gamma}\,\frac{\partial G_{\alpha\beta}}{\partial R_\gamma} = 0, \tag{28}$$

we can replace $\Lambda^d_{\beta\gamma\beta'\gamma'}$ by $\Omega^d_{\beta\gamma\beta'\gamma'} = C_d(\delta_{\beta\beta'}\delta_{\gamma\gamma'}+\delta_{\beta\gamma'}\delta_{\beta'\gamma}+\delta_{\beta\gamma}\delta_{\beta'\gamma'})$ with $C_3=1/15$ and $C_2=1/8$ in the above expression and below.

Analyzing Eq. (27), one can notice that mean-square displacements within time T behave as $\langle\delta\rho^2_\alpha(T)\rangle\propto h(T)$ where

$$h(T) = \int_0^T dt\int_0^{2t} S(\tau)\sigma(\tau)\,d\tau. \tag{29}$$

Thus, at very short times, the motion of tracer particles is ballistic, $h(T)\approx S(0)\sigma(0)T^2$. On the other hand, at long times, $h(T)$ is proportional to T,

$$h(T)\approx T\int_0^\infty S(\tau)\sigma(\tau)\,d\tau, \tag{30}$$

and classical diffusion behavior is observed. According to Eq. (29), this classical regime sets in when $T\gg\max(\tau_m,\tau_{\rm angle})$ where τ_m is the correlation time for the magnitude $m(t)$ of the force dipoles and $\tau_{\rm angle}$ is their orientational correlation time.

The diffusion coefficients are defined by equations $\langle\rho_\alpha(T)\rho_{\alpha'}(T)\rangle = 2D_{\alpha\alpha'}T$. Note that, in addition to the advection due to active force dipoles, passive particles will

also be subject to thermal noise. Therefore, the diffusion coefficients will be given by a sum $D_{\alpha\alpha'} = D_T\delta_{\alpha\alpha'} + D^A_{\alpha\alpha'}$ where D_T is the thermal diffusion coefficient and $D^A_{\alpha\alpha'}$ is the diffusion enhancement caused by the activity of force dipoles. As follows from Eq. (27), we have

$$D^A_{\alpha\alpha'}(\boldsymbol{R}) = \Omega^d_{\beta\gamma\beta'\gamma'}\int \frac{\partial G_{\alpha\beta}(\boldsymbol{R}-\boldsymbol{r})}{\partial r_\gamma}\frac{\partial G_{\alpha'\beta'}(\boldsymbol{R}-\boldsymbol{r})}{\partial r_{\gamma'}}\,c(\boldsymbol{r})\chi(\boldsymbol{r})\,d\boldsymbol{r}, \quad (31)$$

where

$$\chi(\boldsymbol{r}) = \int_0^\infty S(\boldsymbol{r},t)\sigma(t)\,dt. \quad (32)$$

In this equation, we have taken into account that, generally, the activity of force dipoles can depend on the coordinates $\boldsymbol{r}$ (e.g., because the supply of ATP to protein machines is not uniform in the medium). Note that, if the correlation time for the magnitude of force dipoles is much shorter than their orientational correlation time ($\tau_m \ll \tau_{\rm angle}$), Eq. (32) reduces to $\chi(\boldsymbol{r}) = S(\boldsymbol{r})$ where

$$S(\boldsymbol{r}) = \int_0^\infty S(\boldsymbol{r},t)\,dt, \quad (33)$$

where the condition $\sigma(0) = 1$ is taken into account.

Additionally, the mean drift velocity $\bar{V}_\alpha(\boldsymbol{R}^0,T) = \langle d\rho_\alpha/dt\rangle_{\boldsymbol{R}^0}$ at time T for the particle starting its motion at location $\boldsymbol{R}^0$ at time $t = 0$ can be determined. To obtain it, averaging should be performed in Eq. (23). The first term in this equation vanishes after averaging and we obtain

$$\bar{V}_\alpha(\boldsymbol{R}^0,T) = \int d\boldsymbol{r}\,\frac{\partial^2 G_{\alpha\beta}(\boldsymbol{R}^0-\boldsymbol{r})}{\partial r_\gamma \partial r_\delta}\langle\rho_\delta(T)\eta_{\beta\gamma}(T)\rangle. \quad (34)$$

Proceeding in the same way as above for the mean-square displacements, we find that

$$\bar{V}_\alpha(\boldsymbol{R}^0,T) = \Omega^d_{\beta\gamma\beta'\gamma'}\int d\boldsymbol{r}\,\frac{\partial G_{\delta\beta'}(\boldsymbol{R}^0-\boldsymbol{r})}{\partial r_{\gamma'}}\frac{\partial^2 G_{\alpha\beta}(\boldsymbol{R}^0-\boldsymbol{r})}{\partial r_\gamma \partial r_\delta}\,c(\boldsymbol{r}) \times \int_0^T d\tau\, S(T-\tau)\sigma(T-\tau). \quad (35)$$

When $T \gg \max(\tau_m, \tau_{\rm angle})$, this velocity becomes independent of T and we finally obtain

$$\bar{V}_\alpha(\boldsymbol{R}) = \Omega^d_{\beta\gamma\beta'\gamma'}\int \frac{\partial G_{\delta\beta'}(\boldsymbol{R}-\boldsymbol{r})}{\partial r_{\gamma'}}\frac{\partial^2 G_{\alpha\beta}(\boldsymbol{R}-\boldsymbol{r})}{\partial r_\gamma \partial r_\delta}\,c(\boldsymbol{r})\chi(\boldsymbol{r})\,d\boldsymbol{r}. \quad (36)$$

The same derivations can be performed in the case of orientationally ordered force dipoles. As a result, Eqs. (37) and (38) become derived, but, in these equations, the tensor $\Omega^d_{\beta\gamma\beta'\gamma'}$ is replaced by $\overline{N}^d_{\beta\gamma}\overline{N}^d_{\beta'\gamma'}$, so that we have

$$D^A_{\alpha\alpha'}(\boldsymbol{R}) = \overline{N}^d_{\beta\gamma}\overline{N}^d_{\beta'\gamma'}\int \frac{\partial G_{\alpha\beta}(\boldsymbol{R}-\boldsymbol{r})}{\partial r_\gamma}\frac{\partial G_{\alpha'\beta'}(\boldsymbol{R}-\boldsymbol{r})}{\partial r_{\gamma'}}\,c(\boldsymbol{r})\xi(\boldsymbol{r})\,d\boldsymbol{r}, \quad (37)$$

$$\bar{V}_\alpha(\boldsymbol{R}) = \overline{N}^d_{\beta\gamma}\overline{N}^d_{\beta'\gamma'}\int \frac{\partial G_{\delta\beta'}(\boldsymbol{R}-\boldsymbol{r})}{\partial r_{\gamma'}}\frac{\partial^2 G_{\alpha\beta}(\boldsymbol{R}-\boldsymbol{r})}{\partial r_\gamma \partial r_\delta}\,c(\boldsymbol{r})\xi(\boldsymbol{r})\,d\boldsymbol{r}, \quad (38)$$

where

$$\xi(\boldsymbol{r}) = \int_0^\infty S(\boldsymbol{r},t)\,dt. \quad (39)$$

Since diffusion coefficients and the drift velocity are known, the Fokker–Planck equation for the probability density $p(\boldsymbol{r},t)$ of passive particles can be constructed.[13] Because the particles do not interact each with another, the same equation holds for their concentration $n(\boldsymbol{r},t)$, i.e., we have

$$\frac{\partial n}{\partial t} = -\frac{\partial}{\partial r_\alpha}(\bar{V}_\alpha n) + \frac{\partial^2}{\partial r_\alpha \partial r_{\alpha'}}(D_{\alpha\alpha'}n). \quad (40)$$

Note that Eq. (40) can be further rewritten in the classical form of a diffusion equation,

$$\frac{\partial n}{\partial t} = -\frac{\partial}{\partial r_\alpha}(U_\alpha n) + \frac{\partial}{\partial r_\alpha}\left(D_{\alpha\alpha'}\frac{\partial n}{\partial r_{\alpha'}}\right), \quad (41)$$

where

$$U_\alpha = \bar{V}_\alpha - \frac{\partial D_{\alpha\alpha'}}{\partial r_{\alpha'}}. \quad (42)$$

Thus, generally, the activity of force dipoles induces not only the diffusion of passive particles, but also their drift. Both result from advection of particles in fluctuating hydrodynamic fields of active force dipoles and represent therefore an analog of turbulent diffusion effects at high Reynolds numbers.

4. Orientationally Disordered Force Dipoles

In absence of nematic order, general Eqs. (31) and (36) for diffusion coefficients and the drift velocity can be cast into a simpler form. Using explicit expressions (2) and (3) for tensor functions $G_{\alpha\beta}(\boldsymbol{r})$ and performing transformations in these equations, we find that in three-dimensional media ($d = 3$)

$$D^A_{\alpha\alpha'}(\boldsymbol{R}) = \frac{1}{80\pi^2\mu^2}\int \frac{r_\alpha r_{\alpha'}}{r^6}\chi(\boldsymbol{R}+\boldsymbol{r})c(\boldsymbol{R}+\boldsymbol{r})\,d\boldsymbol{r}, \quad (43)$$

$$\bar{V}_\alpha(\boldsymbol{R}) = \frac{1}{40\pi^2\mu^2}\int \frac{r_\alpha}{r^6}\chi(\boldsymbol{R}+\boldsymbol{r})c(\boldsymbol{R}+\boldsymbol{r})\,d\boldsymbol{r}. \quad (44)$$

In two-dimensional media ($d = 2$), one finds[11]

$$D^A_{\alpha\alpha'}(\boldsymbol{R}) = \frac{1}{32\pi^2\mu^2}\int \frac{r_\alpha r_{\alpha'}}{r^4}\chi(\boldsymbol{R}+\boldsymbol{r})c(\boldsymbol{R}+\boldsymbol{r})\,d\boldsymbol{r}, \quad (45)$$

$$\bar{V}_\alpha(\boldsymbol{R}) = \frac{1}{32\pi^2\mu^2}\int \frac{r_\alpha}{r^4}\chi(\boldsymbol{R}+\boldsymbol{r})c(\boldsymbol{R}+\boldsymbol{r})\,d\boldsymbol{r}. \quad (46)$$

These integrals have singularities at $\boldsymbol{r} = \boldsymbol{0}$ (the integrands for the diffusion coefficients diverge as r^{-2} for $d = 3$ and as r^{-1} for $d = 2$). Therefore, a cutoff at some length ℓ_c needs to be introduced. Physically, the cutoff length can be chosen as the sum $\ell_c = \ell_{\rm tracer} + \ell_{\rm dipole}$ of the sizes of a tracer particle and of the object giving rise to a force dipole. Additionally, the integrals have a weak logarithmic divergence at $r \to \infty$ in two-dimensional media; this divergence has the same origin as for the classical diffusion constant in $d = 2$. To avoid such complication, we assume for $d = 2$ that the concentration c of force dipoles (or their activity χ) vanish at $r \to \infty$.

Further transformation can be also performed for the normalized drift velocity $U_\alpha = \bar{V}_\alpha - \partial D_{\alpha\alpha'}/\partial r_{\alpha'}$. Using expressions (43) and (44) and performing partial integration, for $d = 3$ we find that it is determined by a surface integral

$$U_\alpha(\boldsymbol{r}) = -\frac{1}{80\pi^2\mu^2}\int_\Sigma \frac{r_\alpha r_{\alpha'}}{r^6}\chi(\boldsymbol{R}+\boldsymbol{r})c(\boldsymbol{R}+\boldsymbol{r})\,dS_{\alpha'}. \quad (47)$$

Here the integration is performed over the surface Σ that represents a sphere with radius ℓ_c located at the considered point $\boldsymbol{r}$; we employ the notation $d\boldsymbol{S} = \boldsymbol{n}\,dS$ where $\boldsymbol{n}$ is a unit

vector normal to the surface element dS. It can be shown that, in the limit $\ell_c \to 0$, this surface integral yields

$$U_\alpha(\boldsymbol{r}) = \frac{1}{60\pi\mu^2\ell_c}\frac{\partial(\chi(\boldsymbol{r})c(\boldsymbol{r}))}{\partial r_\alpha}. \tag{48}$$

A similar derivation could be performed[11] for $d = 2$ and the result is

$$U_\alpha(\boldsymbol{r}) = \frac{1}{32\pi\mu^2}\frac{\partial(\chi(\boldsymbol{r})c(\boldsymbol{r}))}{\partial r_\alpha}. \tag{49}$$

Note that the last expression does not include the cutoff length. Thus, according to Eq. (41), passive particles will drift along the direction of the increase of χc.

4.1 *Three-dimensional systems*

Suppose that the system is uniform, i.e., $\chi(\boldsymbol{r}) = \text{const.}$ and $c(\boldsymbol{r}) = \text{const.}$ Then, by taking the integral in (43), one finds[9] that diffusion enhancement is isotropic, $D^A_{\alpha\alpha'} = D_A\delta_{\alpha\alpha'}$, and

$$D_A = \frac{\chi c}{60\pi\mu^2\ell_c}. \tag{50}$$

Hence, diffusion of passive tracers will be enhanced in the regions with the higher concentration or the stronger activity of force dipoles. Moreover, as follows from Eq. (48), such regions will also attract passive particles.

If the gradients of χ and c are sufficiently small, the local approximation (50) can be used and the evolution Eq. (41) for the distribution of passive particle takes the form

$$\frac{\partial n}{\partial t} = -\frac{\partial}{\partial r_\alpha}\left[\kappa\frac{\partial(\chi c)}{\partial r_\alpha}n\right] + \frac{\partial}{\partial r_\alpha}\left[(D_T + \kappa\chi c)\frac{\partial n}{\partial r_\alpha}\right], \tag{51}$$

where $\kappa = (60\pi\mu^2\ell_c)^{-1}$. This evolution equation resembles an equation that describes chemotaxis in bacterial populations: the particles tend to move into the regions with the higher χc and to accumulate there. However, the drift of passive particles is not induced by forces applied or generated by them. Instead, it is caused by a gradient in fluid agitation by active elements that cyclically change their shapes.

The drift is counterbalanced by the concentration gradient and finally a stationary distribution of passive particles becomes established. In the local approximation, it is given by[10]

$$n(\boldsymbol{r}) = n_0\left(1 + \frac{\kappa\chi(\boldsymbol{r})c(\boldsymbol{r})}{D_T}\right), \tag{52}$$

where n_0 is the concentration of passive particles in the regions without force dipoles.

The force dipoles correspond to physical objects, such as molecular machines, that are also immersed into the fluid and are free to diffuse. These microscopic objects, like passive tracers, will be also advected in fluctuating flow fields and their diffusion will be enhanced, as described by Eq. (50). Moreover, their drift described by Eq. (48) will also take place. The evolution of the concentration distribution of such objects will be governed by Eq. (51) where n should be replaced by c, so that we obtain[10]

$$\frac{\partial c}{\partial t} = -\frac{\partial}{\partial r_\alpha}\left[\kappa c^2\frac{\partial\chi(\boldsymbol{r})}{\partial r_\alpha}\right] + D_T\frac{\partial^2 c}{\partial r_\alpha^2}. \tag{53}$$

Hence, force dipoles will tend to aggregate in the regions where their activity is increased. The stationary distribution is

$$c(\boldsymbol{r}) = \frac{c_{\max}}{1 + (\kappa/D_T)(\chi_{\max} - \chi(\boldsymbol{r}))}, \tag{54}$$

where $c_{\max}$ is the concentration at the point where $\chi = \chi_{\max}$ (this parameter can be determined from the normalization condition that the total number of force dipoles in the medium is fixed). Note that, as follows from Eq. (53), the activity of force dipoles does not affect their spatial distribution if $\chi(\boldsymbol{r}) = \text{const.}$

The above results were obtained in the local approximation. To discuss how strong nonlocal effects are, we consider a situation when force dipoles occupy only a spherical region of radius R. Depending on the experimental setup, this can be a region where active bacteria are concentrated or an intracellular domain rich with active proteins. Moreover, we assume that, within this region, their activity and concentration are fixed, $\chi = \chi_0$ and $c = c_0$. By taking the integrals in Eq. (43), diffusion coefficients can be determined both inside and outside of the sphere.

We find that nonlocal effects significantly modify the prediction (50) of the local approximation only within a layer with the width about the cutoff length ℓ_c near the surface of the sphere. They also lead to weak diffusion enhancement outside of the sphere, i.e., in the region without force dipoles. When $r \gg R$, diffusion enhancements in the radial ($D^A_\parallel$) and axial ($D^A_\perp$) directions are

$$D^A_\parallel(r) = D_A\frac{\ell_c R^3}{r^4}, \quad D^A_\perp(r) = D_A\frac{\ell_c R^5}{5r^6}, \tag{55}$$

where D_A is the diffusion coefficient inside the sphere given by Eq. (50).

Figure 1(a) shows accumulation of passive particles inside the region occupied by active force dipoles. In this simulation, force dipoles have the concentration distribution

$$c(r) = \frac{1}{2}c_0\left[1 + \tanh\left(-\frac{r-R}{\delta}\right)\right], \tag{56}$$

and hence the drift velocity of passive particles is

$$U(r) = \frac{\kappa c_0}{2\delta}\left[\cosh\left(-\frac{r-R}{\delta}\right)\right]^{-2}. \tag{57}$$

Initially, passive particles are uniformly distributed.[14] We see that gradual aggregation of particles inside the sphere takes place through an "adsorption" process: the particles reaching the boundary are dragged inside the sphere and their concentration near the boundary starts to increase. This process continues until a stationary distribution is achieved where adsorption and evaporation compensate each another.

4.2 *Two-dimensional systems*

The local approximation does not hold at $d = 2$ and nonlocal effects are always present in such systems. Moreover, the integrals in Eqs. (45) and (46) diverge logarithmically at $r \to \infty$ (this is the same divergence as for the classical diffusion coefficient in 2D); hence the estimates cannot be made assuming that an infinite area is uniformly filled with active force dipoles. To avoid this difficulty, one can consider a situation when the force dipoles occupy only a disk area, so that their concentration is constant, $c(\boldsymbol{r}) = c_0$, inside the disk and vanishes outside it. Moreover, it is convenient to assume that the activity of the dipoles is uniform too, $\chi(\boldsymbol{r}) = \chi_0$. With an application to biomembranes with active protein inclu-

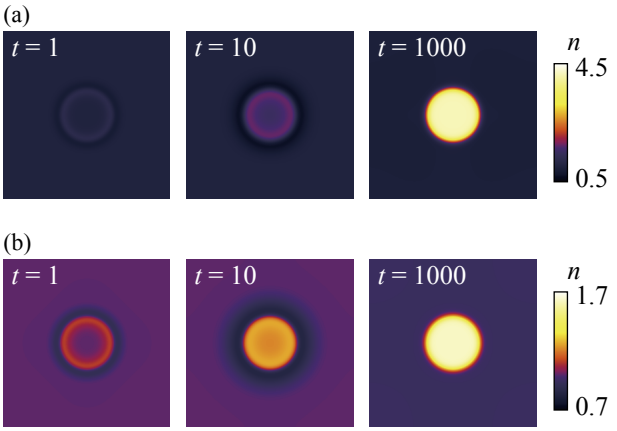

Fig. 1. (Color online) Accumulation of passive particles inside (a) a sphere and (b) a disk occupied by active force dipoles. Consequent snapshots of the concentration distribution are shown. The parameters are $R = 16\ell_c$, $\delta = 2\ell_c$, and $D_0/D_T = 1$; the time unit is ${\ell_c}^2/D_T$; the particles are uniformly distributed with $n = 1$ at $t = 0$.

sions, this situation was analyzed in our previous work.[11] The results of the analysis hold however also in the general case.

Inside the disk (for $r < R - \ell_c$), diffusion enhancement is isotropic and one finds

$$D^A_{\parallel}(r) = D^A_{\perp}(r) = D_0 \ln\left(\frac{\sqrt{R^2 - r^2}}{\ell_c}\right), \tag{58}$$

where

$$D_0 = \frac{\chi_0 c_0}{32\pi\mu^2}. \tag{59}$$

Outside of the disk (for $r > R + \ell_c$), diffusion enhancements in the radial and angular directions are different,

$$D^A_{\parallel}(r) = D_0\left[\ln\left(\frac{r}{\sqrt{r^2 - R^2}}\right) + \frac{R^2}{2r^2}\right], \tag{60}$$

$$D^A_{\perp}(r) = D_0\left[\ln\left(\frac{r}{\sqrt{r^2 - R^2}}\right) - \frac{R^2}{2r^2}\right]. \tag{61}$$

At a large distance from the disk ($r \gg R$), the following asymptotics hold

$$D^A_{\parallel}(r) = \frac{D_0 R^2}{r^2}, \quad D^A_{\perp}(r) = \frac{D_0 R^4}{r^4}. \tag{62}$$

Thus, the angular part of the diffusion coefficient falls much more rapidly with the distance r.

Similar to 3D media, passive particles will accumulate inside the disk. In the final stationary state, the particles are uniformly distributed with concentrations $n_{\rm in}$ and $n_{\rm out}$ inside and outside the disk, respectively. The ratio of the concentrations is[11]

$$\frac{n_{\rm in}}{n_{\rm out}} = \exp\left(\frac{2}{\ln(R/\ell_c) + (1/2) + (2D_T/D_0)}\right). \tag{63}$$

Thus, for example, if $D_0 \gg D_T$ and $R/\ell_c = 16$, this ratio is $n_{\rm in}/n_{\rm out} \simeq 1.84$.

Numerical simulations for evolution of the concentration of passive particles have been performed.[11] Figure 1(b) shows snapshots of the distribution at different subsequent times. In this simulation, force dipoles were distributed as in Eq. (56).[15] As seen in Fig. 1(b), the disk filled with active dipoles is sucking the particles from the region around it. Therefore, the concentration of passive particles starts to increase near the border of the disk. Later on, the particles become uniformly distributed within it.

5. Nematically Ordered Force Dipoles

If oscillating force dipoles are orientationally ordered, flows of passive particles, induced by dipole activity, persist even in the steady state. Although principal effects are similar, the descriptions are different for 2D and 3D media and we consider separately these two cases.

5.1 *Three-dimensional systems*

The nematic order tensor is $\overline{N}^3_{\beta\gamma} = (3\lambda/2)(e^0_\beta e^0_\gamma - \delta_{\beta\gamma}/3)$, where λ is the nematic order parameter and $\boldsymbol{e}^0$ defines the common orientation of the dipoles. The diffusion coefficients and the drift velocity are given by Eqs. (37) and (38). Note that, due to identity $\partial G_{\alpha\beta}/\partial r_\beta = 0$, the factor $\overline{N}^3_{\beta\gamma}\overline{N}^3_{\beta'\gamma'}$ in these equations can be replaced by $(3\lambda/2)^2 e^0_\beta e^0_\gamma e^0_{\beta'} e^0_{\gamma'}$. Moreover, the direction of the vector $\boldsymbol{e}^0$ can be chosen as the direction of the first coordinate axis in the reference frame. With such notations, we have

$$D^A_{\alpha\alpha'}(\boldsymbol{R}) = \int \frac{\partial G_{\alpha 1}(\boldsymbol{R} - \boldsymbol{r})}{\partial r_1}\frac{\partial G_{\alpha' 1}(\boldsymbol{R} - \boldsymbol{r})}{\partial r_1} s(\boldsymbol{r})c(\boldsymbol{r})\, d\boldsymbol{r} \tag{64}$$

$$= \frac{1}{64\pi^2\mu^2}\int (r^2 - 3{r_1}^2)^2 \frac{r_\alpha r_{\alpha'}}{r^{10}} s(\boldsymbol{R} + \boldsymbol{r})c(\boldsymbol{R} + \boldsymbol{r})\, d\boldsymbol{r}, \tag{65}$$

$$\bar{V}_\alpha(\boldsymbol{R}) = \int \frac{\partial G_{\delta 1}(\boldsymbol{R} - \boldsymbol{r})}{\partial r_1}\frac{\partial^2 G_{\alpha 1}(\boldsymbol{R} - \boldsymbol{r})}{\partial r_\delta \partial r_1} s(\boldsymbol{r})c(\boldsymbol{r})\, d\boldsymbol{r} \tag{66}$$

$$= \frac{1}{32\pi^2\mu^2}\int (r^2 - 3{r_1}^2)^2 \frac{r_\alpha}{r^{10}} s(\boldsymbol{R} + \boldsymbol{r})c(\boldsymbol{R} + \boldsymbol{r})\, d\boldsymbol{r}, \tag{67}$$

$$U_\alpha(\boldsymbol{r}) = \kappa M_{\alpha\alpha'}\frac{\partial(s(\boldsymbol{r})c(\boldsymbol{r}))}{\partial r_\alpha}, \tag{68}$$

where M is a diagonal matrix, $M_{\alpha\alpha'} = M^{(\alpha)}\delta_{\alpha\alpha'}$, with $M^{(1)} = 11/7$, and $M^{(2)} = M^{(3)} = 5/7$, and

$$s(\boldsymbol{r}) = \frac{9\lambda^2}{4}\xi(\boldsymbol{r}) = \frac{9\lambda^2}{4}\int_0^\infty S(\boldsymbol{r}, t)\, dt. \tag{69}$$

Similar to the orientationally disordered 3D case, local approximation can be used again and we obtain

$$D^A_{\alpha\alpha'}(\boldsymbol{r}) = \kappa M_{\alpha\alpha'} s(\boldsymbol{r})c(\boldsymbol{r}), \tag{70}$$

$$\bar{V}_\alpha(\boldsymbol{r}) = 2\kappa M_{\alpha\alpha'}\frac{\partial(s(\boldsymbol{r})c(\boldsymbol{r}))}{\partial r_{\alpha'}}. \tag{71}$$

Thus, diffusion is anisotropic: it is enhanced stronger along the orientation line of force dipoles than in the directions orthogonal to this line. Note also that the drift velocity is not parallel to the gradient $\nabla(sc)$.

The equation for concentration of passive particles is

$$\frac{\partial n}{\partial t} = -\frac{\partial}{\partial r_\alpha}\left[\kappa M^{(\alpha)}\frac{\partial(sc)}{\partial r_\alpha} n\right] + \frac{\partial}{\partial r_\alpha}\left[(D_T + \kappa M^{(\alpha)} sc)\frac{\partial n}{\partial r_\alpha}\right]. \tag{72}$$

It is equivalent to the conservation equation

$$\frac{\partial n}{\partial t} + \frac{\partial j_\alpha}{\partial r_\alpha} = 0, \tag{73}$$

for the flux

$$j_\alpha(\boldsymbol{r},t) = \kappa M^{(\alpha)} \frac{\partial(sc)}{\partial r_\alpha} n - (D_T + \kappa M^{(\alpha)} sc) \frac{\partial n}{\partial r_\alpha}. \quad (74)$$

In contrast to the orienationally disordered case, this flux does not vanish in the steady state.

The existence of circulating fluxes in the steady state can be demonstrated by considering a situation where force dipoles occupy a sphere of radius R and are absent outside of it, $c(\boldsymbol{r}) = c_0$ for $0 < r < R$ and $c(\boldsymbol{r}) = 0$ for $r > R$; moreover, we assume $s(\boldsymbol{r}) = s_0$. Suppose that the dipole activity is weak, $\kappa s_0 c_0 \ll D_T$. In this limiting case, the distribution of passive particles will be only slightly affected by force dipoles, so that $n(\boldsymbol{r}) \approx n_0$. Then, the flux in the steady state is

$$j_\alpha \approx -\kappa s_0 c_0 n_0 M^{(\alpha)} \delta(r-R)\hat{r}_\alpha, \quad (75)$$

where $\hat{\boldsymbol{r}} = \boldsymbol{r}/r$. This flux is present only on the surface of the sphere, it varies over it and has both the radial and the tangential components. Such surface flux induces weak circulating flows of particles both inside the sphere and in the bulk.

Numerical simulations were performed assuming that concentration distribution of force dipoles is smooth and given by Eq. (56) and that $s(\boldsymbol{r}) = s_0$.[16] Figures 2(a) and 2(b) show the distribution $n(\boldsymbol{r})$ in the final steady state. We see that particles become accumulated inside the sphere. However, their distribution is not uniform inside and outside of the sphere. This is because of the circulating flows that are present in the steady state. The distribution of magnitude $j(\boldsymbol{r})$ of the flux is shown in Fig. 2(c) and the stream lines are displayed in Fig. 2(d). The particles enter the sphere through the poles and leave it over the equator. It can be shown that the fluxes outside of the sphere are of the order $D_T/(\kappa s_0 c_0)$ when $\kappa s_0 c_0 \gg D_T$.

5.2 *Two-dimensional systems*

The nematic tensor in 2D systems is $\overline{N}^2_{\beta\gamma} = 2\lambda(e^0_\beta e^0_\gamma - \delta_{\beta\gamma}/2)$, the diffusion coefficients and the drift velocity are determined by the integrals (64) and (66) with

$$s(\boldsymbol{r}) = 4\lambda^2 \xi(\boldsymbol{r}) = 4\lambda^2 \int_0^\infty S(\boldsymbol{r},t)\, dt. \quad (76)$$

The local approximation is not applicable in this case. As previously, for the disordered dipoles, the integrals (64) and (66) can be cast into a more simple form

$$D^A_{\alpha\alpha'}(\boldsymbol{R}) = \frac{1}{16\pi^2\mu^2} \int ({r_1}^2 - {r_2}^2)^2 \frac{r_\alpha r_{\alpha'}}{r^8} s(\boldsymbol{R}+\boldsymbol{r}) c(\boldsymbol{R}+\boldsymbol{r})\, d\boldsymbol{r}, \quad (77)$$

$$\bar{V}_\alpha(\boldsymbol{R}) = \frac{1}{16\pi^2\mu^2} \int ({r_1}^2 - {r_2}^2)^2 \frac{r_\alpha}{r^8} s(\boldsymbol{R}+\boldsymbol{r}) c(\boldsymbol{R}+\boldsymbol{r})\, d\boldsymbol{r}, \quad (78)$$

where the first axis is chosen as the orientation line of the force dipoles. These expressions can be used to determine the diffusion constants and the drift velocities for any spatial distribution of force dipoles. For the drift velocity, we have

$$U_\alpha(\boldsymbol{r}) = \frac{1}{32\pi\mu^2} \frac{\partial(s(\boldsymbol{r})c(\boldsymbol{r}))}{\partial r_\alpha}, \quad (79)$$

which is the same expression as in the disordered case.

As an example, we consider a situation when the dipoles are uniformly distributed inside a disk of radius R and are absent outside of it; we also assume $s(\boldsymbol{r}) = s_0$. In this case, calculations yield the following results:

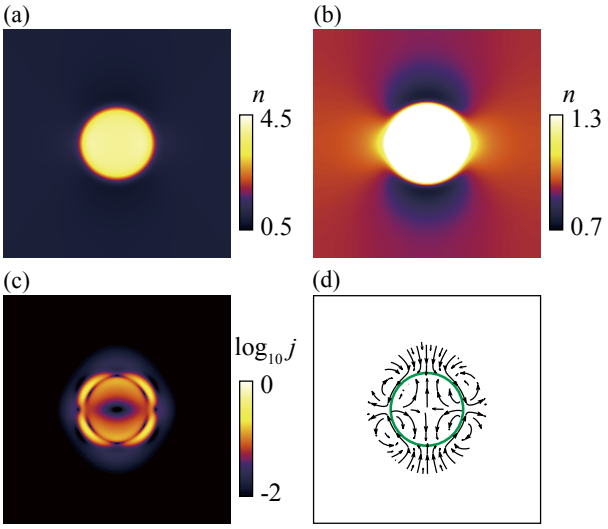

Fig. 2. (Color online) Distribution of passive particles (a, b) and their fluxes (c, d) in the steady state of a 3D system with orientationally ordered force dipoles that occupy a sphere in the center ($t = 1000$). Part (b) shows the distribution enhanced in the region of low concentrations. The logarithm $\log_{10} j(\boldsymbol{r})$ of the local magnitude of the fluxes and their stream lines are displayed in (c) and (d). In panel (d), the stream lines in the region for $\log_{10} j(\boldsymbol{r}) > -2$ are shown. The vertical direction corresponds to the orientation line of force dipoles (r_1-axis). The parameters are $R = 16\ell_c$, $\delta = 2\ell_c$, $c_0 = 1$, and $s_0 = 1$.

Inside the disk ($r < R - \ell_c$), we have

$$D^A_\parallel(\boldsymbol{r}) = D^A_\perp(\boldsymbol{r}) = D_0 \ln\left(\frac{\sqrt{R^2 - r^2}}{\ell_c}\right), \quad (80)$$

which is the same as for the random alignment.

Outside of the disk, diffusion is anisotropic and, moreover, cross diffusion takes place. The components of the diffusion tensor outside of the disk ($r > R + \ell_c$) are

$$D^A_\parallel(\boldsymbol{r}) = D_0\left[\ln\left(\frac{r}{\sqrt{r^2 - R^2}}\right) + \frac{R^2}{2r^2} + \frac{R^2(12r^4 - 21r^2R^2 + 10R^4)}{12r^6}\cos 4\theta\right], \quad (81)$$

$$D^A_\perp(\boldsymbol{r}) = D_0\left[\ln\left(\frac{r}{\sqrt{r^2 - R^2}}\right) - \frac{R^2}{2r^2} + \frac{R^4(3r^2 - 10R^2)}{12r^6}\cos 4\theta\right], \quad (82)$$

and

$$D^A_{\rm cross}(\boldsymbol{r}) = D_0 \frac{R^4(6r^2 - 5R^2)}{6r^6} \sin 4\theta. \quad (83)$$

Here, we set $\boldsymbol{r} = (r\cos\theta, r\sin\theta)$ and the diffusion tensor is written as

$$D^A_{\alpha\beta}(\boldsymbol{r}) = (D_T + D^A_\perp(\boldsymbol{r}))\delta_{\alpha\beta} + (D^A_\parallel(\boldsymbol{r}) - D^A_\perp(\boldsymbol{r}))\frac{r_\alpha r_\beta}{r^2} + D^A_{\rm cross}(\boldsymbol{r})\left(\iota_{\alpha\gamma}\frac{r_\beta r_\gamma}{r^2} + \iota_{\beta\gamma}\frac{r_\alpha r_\gamma}{r^2}\right), \quad (84)$$

with $\iota_{\alpha\beta}$ defined as $\iota_{12} = -1$, $\iota_{21} = 1$, and $\iota_{11} = \iota_{22} = 0$.

Furthermore, temporal evolution of the distribution of passive particles and this distribution in the final steady state can be obtained by integrating Eq. (40). We have performed

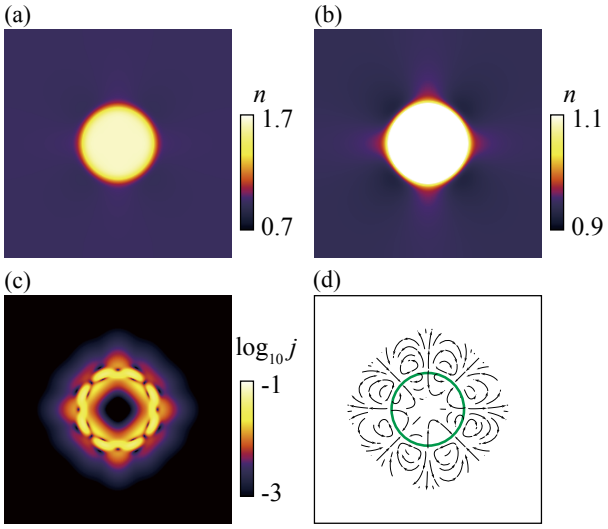

Fig. 3. (Color online) Distribution of passive particles (a, b) and their fluxes (c, d) in the steady state of a 2D system with orientationally ordered force dipoles that occupy a circle in the center ($t = 1000$). Part (b) shows the distribution enhanced in the region of low concentrations. The logarithm $\log_{10} j(\boldsymbol{r})$ of the local magnitude of the fluxes and their stream lines are displayed in (c) and (d). In panel (d), the stream lines in the region for $\log_{10} j(\boldsymbol{r}) > -3$ are shown. The horizontal direction corresponds to the orientation line of force dipoles (r_1-axis). The parameters are $R = 16\ell_c$, $\delta = 2\ell_c$, $c_0 = 1$, and $s_0 = 1$.

the numerical integration assuming that the distribution of force dipoles is fixed and given by Eq. (56). We also assume that $s(\boldsymbol{r}) = s_0$. The simulations started with a uniform distribution of passive particles.[17)]

Figure 3 presents the results for the final distribution of passive particles and for the flux. We see that there are significant differences from the three-dimensional case (cf. Fig. 2). While the 3D distributions had a two-fold symmetry in the median cross-section, the symmetry is four-fold in 2D. Now the particles are leaving the disk both along the orientation line of force dipoles and along the line orthogonal to it.

6. Discussion and Conclusions

In oscillatory active nematics, a variety of hydrodynamic effects can be observed. The activity of force dipoles, corresponding to the elements that cyclically change their shapes, leads to stirring of the fluid and generation of non-thermal fluctuating flows within it. Passive particles are advected by such fluctuating flows and, as a result, their diffusion is enhanced. This phenomenon is analogous to turbulent diffusion, but takes place at low Reynolds numbers where inertial effects and nonlinearities are absent. Furthermore, directed drift of tracer particles is induced if the spatial distribution of force dipoles (or of their activity) is non-uniform. The effects are local in 3D systems and nonlocal in 2D. Depending on a system, orientational ordering in oscillatory active nematics can arise. As we have seen, hydrodynamic behavior is sensitive to the nematic order in populations of force dipoles.

An important consequence is that passive particles are driven by fluctuating flows into the regions with the high concentration or activity of force dipoles. This leads to a non-equilibrium redistribution of passive particles in the medium, maintained only as long as the activity of force dipoles persists. This provides a possibility to control spatial distributions of particles by purely hydrodynamic means, without applying any force fields.

In original publications,[9,10)] hydrodynamical effects in oscillatory active nematics were studied under an assumption that orientations and positions of active force dipoles did not change significantly within a cycle, so that the dipoles could be treated as immobile. In the present article, we allowed for orientational fluctuations in the disordered state. Furthermore, systems with the orientational nematic order were also analyzed.

The considered phenomena are important for biological cells. It was shown by in vivo experiments that active non-thermal noise dominates transport phenomena in the cytoplasm.[18)] Such non-thermal noise can be due to molecular motors operating on the cytoskeleton[18,19)] or be caused by the metabolic activity inside the cell.[20)] To analyze such effects, viscoelastic properties of the cytoplasm have to be taken into account.[12)] Moreover, biological membranes typically include a large number of proteins and many such inclusions operate as molecular machines, cyclically changing their shapes. Active proteins are typically confined within protein rafts. On the length scales shorter than about a micrometer, lipid bilayers behave as 2D fluids[21,22)] and, therefore, fluctuating lipid flows are induced when inclusions change their shapes. Their activity enhances diffusion and induces redistribution of particles over the membrane.[11)]

Experiments with suspensions of synthetic molecular machines[4)] or with the oscillating dumbbells can be performed too. Moreover, similar effects are expected for populations of microorganisms that, while not acting as swimmers, reciprocally change their shapes. With this respect, it should be noted that in bacterial layers formed by swimming microorganisms, diffusion can be enhanced by a factor up to 100;[23)] these effects have been theoretically investigated.[24–26)]

Our analysis was based on a number of simplifications. Energetic interactions between the particles were not taken into account, although they might become important when accumulation of the particles in some regions occurs. We have also not taken into account fluctuation effects, even though they may become essential on short length scales. Moreover, only the situations with a perfect orientational order or without any order were considered by us. The respective theory extensions are the task for some future work.

Acknowledgments We are grateful to R. Kapral for stimulating discussions. This work was supported by JSPS KAKENHI Grant Nos. JP25103008, JP26520205, and JP15K05199. This work was supported in part by the Core-to-Core Program "Nonequilibrium dynamics of soft matter and information" (Grant No. 23002) to Y.K. and H.K., and by the EU program "Nonequilibrium dynamics of soft and active matter" (Grant No. PIRSES-GA-2011-295243) to A.M.

*mik@fhi-berlin.mpg.de

1) P. G. De Gennes and J. Prost, *The Physics of Liquid Crystals* (Oxford University Press, Oxford, U.K., 1974).
2) V. Balzani, A. Credi, F. R. Raymo, and J. F. Stoddart, Angew. Chem., Int. Ed. **39**, 3348 (2000).

3) J. Wang, *Nanomachines: Fundamentals and Applications* (Wiley-VCH, Weinheim, 2013).
4) V. Balzani, M. Clemente-Leon, A. Credi, B. Ferrer, M. Venturi, A. H. Flood, and J. F. Stoddart, Proc. Natl. Acad. Sci. U.S.A. **103**, 1178 (2006).
5) N. Koumura, R. W. J. Zijlstra, R. A. van Delden, N. Harada, and B. L. Feringa, Nature **401**, 152 (1999).
6) R. A. van Delden, M. K. J. ter Wiel, M. M. Polard, J. Vicario, N. Koumura, and B. L. Feringa, Nature **437**, 1337 (2005).
7) E. M. Purcell, Am. J. Phys. **45**, 3 (1977).
8) E. Lauga and T. R. Powers, Rep. Prog. Phys. **72**, 096601 (2009).
9) A. S. Mikhailov and R. Kapral, Proc. Natl. Acad. Sci. U.S.A. **112**, E3639 (2015).
10) R. Kapral and A. S. Mikhailov, Physica D **318–319**, 100 (2016).
11) Y. Koyano, H. Kitahata, and A. S. Mikhailov, Phys. Rev. E **94**, 022416 (2016).
12) K. Yasuda, R. Okamoto, S. Komura, and A. S. Mikhailov, Europhys. Lett. **117**, 38001 (2017).
13) A. Risken, *The Fokker–Planck Equation* (Springer, Berlin, 1984).
14) Numerical simulations were performed with the Euler method using Eqs. (40), (43), and (44). The advection and diffusion terms were calculated with the explicit method. Time step was 10^{-4} and the spatial mesh size was 0.4. Axial symmetry was assumed and the calculation was performed in the median plane.
15) Numerical simulations were performed with the Euler method using Eqs. (40), (45), and (46). The advection and diffusion terms were calculated with the explicit method. Time step was 10^{-4} and the spatial mesh size was 0.4.
16) Numerical simulations were performed with the Euler method using Eqs. (40), (65), and (67). The advection and diffusion terms were calculated with the explicit method. Time step was 10^{-4} and the spatial mesh size was 0.4. Axial symmetry was assumed and the calculation was performed in the median plane.
17) Numerical simulations were performed with the Euler method using Eqs. (40), (77), and (78). The advection and diffusion terms were calculated with the explicit method. Time step was 10^{-4} and the spatial mesh size was 0.4.
18) M. Guo, A. J. Ehrlicher, M. H. Jensen, M. Renz, J. R. Moore, R. D. Goldman, J. Lippincott-Schwartz, F. C. Mackintosh, and D. A. Weitz, Cell **158**, 822 (2014).
19) É. Fodor, M. Guo, N. S. Gov, P. Visco, D. A. Weitz, and F. van Wijland, Europhys. Lett. **110**, 48005 (2015).
20) B. R. Parry, I. V. Surovtsev, M. T. Cabeen, C. S. O'Hern, E. R. Dufresne, and C. Jacobs-Wagner, Cell **156**, 183 (2014).
21) P. G. Saffman and M. Delbrück, Proc. Natl. Acad. Sci. U.S.A. **72**, 3111 (1975).
22) H. Diamant, J. Phys. Soc. Jpn. **78**, 041002 (2009).
23) X.-L. Wu and A. Libchaber, Phys. Rev. Lett. **84**, 3017 (2000).
24) Y. Hatwalne, S. Ramaswamy, M. Rao, and R. A. Simha, Phys. Rev. Lett. **92**, 118101 (2004).
25) P. T. Underhill and M. D. Graham, Phys. Fluids **23**, 121902 (2011).
26) J. P. Hernandez-Ortiz, P. T. Underhill, and M. D. Graham, J. Phys.: Condens. Matter **21**, 204107 (2009).

Alexander S. Mikhailov was born in Russia in 1950. He obtained his Diploma (1973), Ph.D. (1976) and Dr.Sc. (1984) degrees from the Lomonosov Moscow State University. He works in Germany since 1990, first as a guest professor in the University of Stuttgart (1990–1991). Starting from 1995, he is a staff scientist (professor) and a group leader in the Department of Physical Chemistry of the Fritz Haber Institute in Berlin. He has been a guest professor in the Hokkaido, Kyoto and Hiroshima universities; and was awarded the International Solvay Chair in Chemistry in 2009. He is an editor of *Progress of Theoretical and Experimental Physics*. He has been working on a broad range of topics in theoretical chemical and biological physics, nonlinear dynamics and network science.

Yuki Koyano was born in Chiba, Japan in 1991. She obtained her B.Sci. (2013) and her M.Sci. (2015) from Chiba University. She is an doctor course student (2015–) at Department of Physics, Chiba University. She has been working on nonlinear physics, especially on self-propelled systems.

Hiroyuki Kitahata was born in Osaka, Japan in 1978. He obtained his B.Sci. (2001), his M.Sci. (2003), and his D.Sci. (2006) from Kyoto University. He was an assistant professor (2004–2008) at Department of Physics, Kyoto University, and a lecturer (2008–2010) and an associate professor (2011–) at Department of Physics, Chiba University. He is a head editor of the *Journal of the Physical Society of Japan*. He has been working on nonlinear physics, especially on active matter and spatio-temporal self-organization.